


# Polyethylene Glycol-Coated Graphene Oxide Loaded with Erlotinib as an Effective Therapeutic Agent for Treating Nasopharyngeal Cancer Cells

This article was published in the following Dove Press journal:  
*International Journal of Nanomedicine*

Ming-Ying Lan <sup>1,2</sup>  
Yen-Bin Hsu <sup>1,2</sup>  
Ming-Chin Lan<sup>3,4</sup>  
Jyh-Ping Chen <sup>5-8</sup>  
Yu-Jen Lu <sup>9</sup>

<sup>1</sup>Department of Otolaryngology-Head and Neck Surgery, Taipei Veterans General Hospital, Taipei, Taiwan; <sup>2</sup>School of Medicine, National Yang-Ming University, Taipei, Taiwan; <sup>3</sup>Department of Otolaryngology-Head and Neck Surgery, Taipei Tzu Chi Hospital, Buddhist Tzu Chi Medical Foundation, New Taipei City, Taiwan; <sup>4</sup>School of Medicine, Tzu Chi University, Hualien, Taiwan; <sup>5</sup>Department of Chemical and Materials Engineering, Chang Gung University, Taoyuan, Taiwan; <sup>6</sup>Department of Plastic and Reconstructive Surgery and Craniofacial Research Center, Chang Gung Memorial Hospital, Taoyuan, Taiwan; <sup>7</sup>Research Center for Food and Cosmetic Safety, Research Center for Chinese Herbal Medicine, College of Human Ecology, Chang Gung University of Science and Technology, Taoyuan, Taiwan; <sup>8</sup>Department of Materials Engineering, Ming Chi University of Technology, Taipei, Taiwan; <sup>9</sup>Department of Neurosurgery, Chang Gung Memorial Hospital Linkou Medical Center and College of Medicine, Chang Gung University, Taoyuan, Taiwan

Correspondence: Yu-Jen Lu  
Department of Neurosurgery, Chang Gung Memorial Hospital Linkou Medical Center and College of Medicine, Chang Gung University, Taoyuan, Taiwan  
Email alexlu0416@gmail.com

Jyh-Ping Chen  
Department of Chemical and Materials Engineering, Chang Gung University, Taoyuan, Taiwan  
Email jpchen@mail.cgu.edu.tw

**Introduction:** Nasopharyngeal carcinoma (NPC) is a common cancer in southern China and Taiwan, and radiation therapy combined with or without chemotherapy is its mainstay treatment. Although it is highly sensitive to radiotherapy, local recurrence and distant metastasis remain difficult unsolved problems. In recent years, graphene oxide (GO) has been found to be a promising novel anticancer drug carrier. Here, we present our designed functionalized GO, polyethylene glycol-coated GO (GO-PEG), as a drug carrier, which was loaded with erlotinib and showed promising anticancer effects on NPC cells.

**Methods:** The effects of GO-PEG-erlotinib on the proliferation, migration, and invasion of NPC cells were investigated by WST-8 assay, wound healing assay, and invasion assay, respectively. RNA sequencing was conducted and analyzed to determine the molecular mechanisms by which GO-PEG-erlotinib affects NPC cells.

**Results:** Our results showed that GO-PEG-erlotinib reduced NPC cell viability in a dose-dependent manner and also inhibited the migration and invasion of NPC cells. The RNA sequencing revealed several related molecular mechanisms.

**Conclusion:** GO-PEG-erlotinib effectively suppressed NPC cell proliferation, migration, and invasion, likely by several mechanisms. GO-PEG-erlotinib may be a potential therapeutic agent for treating NPC in the future.

**Keywords:** nasopharyngeal carcinoma, anti-cancer, graphene oxide, erlotinib, drug carrier

## Introduction

Nasopharyngeal carcinoma (NPC) is very rare in western countries but is one of the most common cancers in southern Asian with annual incidence around 20–30/100,000.<sup>1,2</sup> Due to its deep location inside the nasal cavity and vague symptoms, most NPC patients have been diagnosed at an advanced stage.<sup>2</sup> The etiology of NPC has been proved to be closely related to several factors, including genetic, Epstein-Barr virus exposure, environmental, and dietary factors.<sup>1-4</sup> During development of the disease, viral infection and multiple somatic genetic and epigenetic changes synergistically disrupt normal cell function, thus contributing to NPC pathogenesis.<sup>3-8</sup> Radiotherapy is the foundation of curative treatment for NPC, and chemotherapy is usually combined with radiotherapy for advanced cases.<sup>9</sup> Although NPC is highly radiosensitive and chemosensitive with an optimal 5-year survival of over 80%, the treatment of patients with locoregionally advanced disease remains problematic due to locoregional failure and distant metastasis. Besides, patients often suffer from systemic toxicity or related complications of

chemotherapy. To reach a better outcome for NPC treatment, the refinement of current treatment modalities is of importance.

The recent development of novel materials, especially nanoparticles, having the advantages of large surface area-to-volume ratio and small size, enables them to carry small compounds with high efficiency. Graphene and its derivatives have drawn much attention in pharmaceutical sciences as carriers for targeted drug delivery in cancer diagnosis and treatment.<sup>10–13</sup> Graphene is an allotrope of carbon in the form of a one-atom-thick, two-dimensional, atomic-scale, hexagonal lattice, with high thermal conductivity, excellent mechanical properties, and large surface areas.<sup>14</sup> There are several members of the graphene family, including graphene oxide (GO), reduced graphene oxide (RGO), and graphene quantum dots (GQDs), that have been used in materials science, nanotechnology, and biomedicine. The combination of biomolecules, such as DNA, peptides, proteins, enzymes, carbohydrates, and viruses, with graphene-based materials offers a promising method to fabricate novel graphene-biomolecule hybrid nanomaterials with unique functions in drug delivery, cancer treatment, tissue engineering, biosensors, bioimaging, energy materials, and other nanotechnological applications.<sup>15–20</sup>

Erlotinib, a tyrosine kinase inhibitor (TKI) acting on the epidermal growth factor receptor (EGFR), was demonstrated in 2004 to be effective for locally advanced or metastatic non-small cell lung cancer (NSCLC) and, in combination with gemcitabine, for locally advanced or metastatic pancreatic cancer.<sup>21</sup> Currently, there is little information regarding its usage in NPC. Previously, an *in vitro* study showed that erlotinib has a role as an enhancer of radiation therapy in NPC.<sup>22</sup> However, a Phase II trial conducted on patients with recurrent and/or metastatic NPC revealed no efficacy of erlotinib as maintenance therapy after gemcitabine-platinum chemotherapy.<sup>23</sup>

Our previous works have prioritized several crucial NPC targets and identified many potential drugs for treating NPC.<sup>24,25</sup> Erlotinib is one of our potential drugs and was selected to be loaded on specific functionalized graphene to investigate its anticancer effect. The RNA sequencing was conducted to reveal related molecular mechanisms. The goal is to develop drugs with better anticancer activity but lower toxicity for possible future clinical applications in NPC patients.

## Materials and Methods

### Preparation of Graphene Oxide (GO)

The raw materials of graphite platelet (model xGnP) measuring 100  $\mu\text{m}$  in width and 5–15 nm in thickness were obtained from XG Sciences Inc (East Lansing, MI). Acrylic acid, potassium persulfate, sulfuric acid ( $\text{H}_2\text{SO}_4$ , 98%), sodium sulfate ( $\text{Na}_2\text{SO}_4$ ), potassium permanganate ( $\text{KMnO}_4$ ), hydrogen peroxide solution ( $\text{H}_2\text{O}_2$ ), and ammonia solution were purchased from Showa Chemical Co (Tokyo, Japan). Preparation of GO followed the modified Hummers' method (Figure 1).<sup>26</sup> One gram of graphite platelet and 23 mL of  $\text{H}_2\text{SO}_4$  (98%) were added into a 250 mL flask under magnetic stirring for 12 hours, followed by slow addition of 3 g of  $\text{KMnO}_4$  in an ice bath while keeping the temperature below 20°C. After stirring for 30 minutes, the flask was heated to 35–40°C and continually stirred for 30 minutes. The temperature of the solution was increased to 65–80°C with continued stirring for 45 minutes, followed by addition of 46 mL of deionized water. Then, the temperature of the solution was increased to 98–105°C and stirred for 30 minutes. After cooling for 1 hour at room temperature, 140 mL of deionized water and 10 mL 10%  $\text{H}_2\text{O}_2$  were added to the solution and incubated for 5 minutes at 35–40°C. The solution was centrifuged at 10,000 rpm and washed using 5% HCl solution 2–3 times. Then, deionized water was used to wash the precipitate several times to neutralize it. The precipitate was collected and subject to ultrasonication using an Ultrasonic Liquid Processor 2020 from Misonix (Farmingdale, NY) and filtered with Acrodisc 25 mm syringe filters (0.2  $\mu\text{m}$  Supor membrane). GO collected in the filtrate was subjected to further modification.

### Preparation of PEGylated GO (GO-PEG)

GO-polyethylene glycol (GO-PEG) was made following the method below. Briefly, the PBS was added to GO solution and sonicated for 1 hour. After cooling at room temperature, DSPE-PEG- $\text{CH}_3$  was added to the solution. The solution was then sonicated for 1 hour in an ice bath. Finally, the solution was centrifuged at high speed for 1 hour and the supernatant was removed. All GO materials were then dispersed in sterilized deionized water to prepare the stock solution (0.5 or 1 mg/mL) for later characterization and experiments.

### Characterization of GO Materials

- (i) Fourier transform infrared spectroscopy (FTIR)

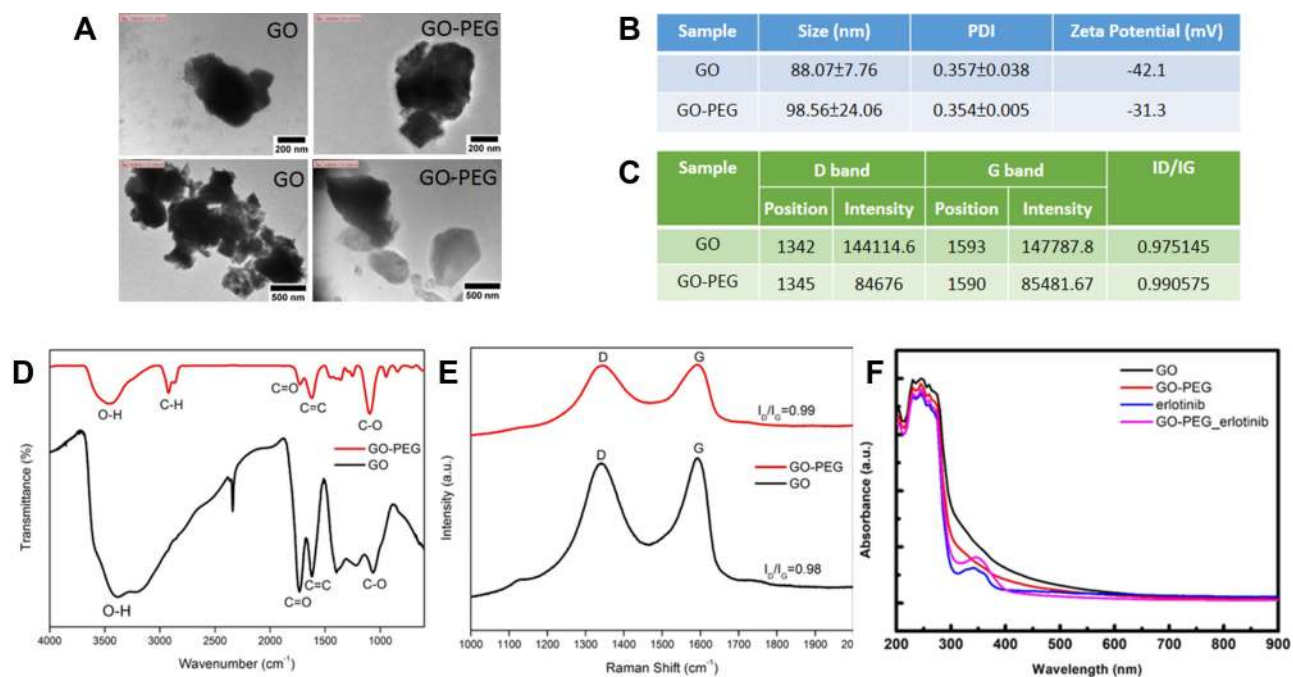


**Figure 1** Characterizations of GO and GO-PEG. **(A)** TEM images of GO and GO-PEG. **(B)** The table lists the measurements of size and zeta potential of GO and GO-PEG analyzed by DLS. **(C)** The intensity of D and G band of GO and GO-PEG in Raman spectra. **(D)** The infrared spectrum of GO and GO-PEG by FTIR shows that PEG was successfully conjugated on GO. **(E)** Raman spectra of GO and GO-PEG. **(F)** Absorbance of GO, GO-PEG, erlotinib, and GO-PEG-erlotinib analyzed by UV-Vis spectrophotometer.

**Abbreviation:** PDI, polydispersity index.

FTIR (Bruker Tensor 27) was used to obtain an infrared spectrum of absorption or emission of the GO and functionalized GO materials.

#### (ii) Dynamic light scattering (DLS) and zeta potential

The sizes of GO and GO-PEG were respectively measured by the zetasizer (Zetasizer Nano ZS90, Malvern).

#### (iii) TEM

Transmission electron microscopy (TEM; JEM-2100, JEOL, Japan) was utilized to determine the structure of the GO materials. The TEM samples were prepared by depositing a small drop of solution onto a carbon-coated copper electron microscopy grid and then dried at room temperature.

#### (iv) Raman spectroscopy

Raman spectra were collected using a Micro-Raman Spectrometer (PTT-EL) equipped with a 532nm laser and a 10X objective. The Raman spectra integration time was 20 sec for each location.

## Drug Loading Study

To prepare GO-PEG loaded with erlotinib (GO-PEG-erlotinib), 200 µg erlotinib was mixed with different concentrations of GO-PEG in 1 mL ddH<sub>2</sub>O. The suspension was rotated at 35 rpm at room temperature overnight and then centrifuged for 1 hour. The supernatant was removed and the concentration of erlotinib in the solution was analyzed by UV-Vis Spectrophotometer (Beckman Coulter DU730) at 735, 333, and 371 nm. The weight of drug loaded on GO-PEG was calculated by mass balance from the amount of drug initially added and the amount of drug in the supernatant. The drug entrapment efficiency (EE) (%) is defined as (weight of drug loaded on GO-PEG / weight of drug initially added) × 100. The drug loading efficiency (LE) (%) is defined as (weight of drug loaded on GO-PEG / weight of GO-PEG) × 100.

## Drug Release Study

GO-PEG-erlotinib was placed into the microtubes with 1 mL phosphate-buffered saline (PBS) at pH 7.4 and 5.5, respectively. The drug release was assumed to start as soon as the microtubes were placed into the incubator at 37°C. The microtube was under constant shaking. At particular time intervals, all supernatant was withdrawn from the

microtube for characterization after centrifugation and washing. The microtube was replenished with the same volume of PBS to continue the drug release study. The concentration of erlotinib released from the functionalized GO-PEG-erlotinib complex was determined using a UV-Vis Spectrophotometer (Beckman Coulter DU730). The drug release percentage was calculated from the cumulative amount of drug released after normalizing with amount of loaded drug.

## Cellular Uptake Study

To determine intracellular uptake of GO-PEG, NPC TW01 cells (10,000 cells/mL) were cultured in 2 mL DMEM supplemented with 10% FBS in 35 mm diameter plates. Cells were grown in a humidified incubator at 37°C under 5% CO<sub>2</sub> for 48 hours. To prepare fluorescent GO-PEG, 95  $\mu$ L of 2 mg/mL FITC-NHS (5/6-carboxyfluorescein succinimidyl ester) was mixed with 1 mL of 1 mg/mL GO-PEG solution and then vortexed at 25°C for 1 hour in the dark. The above solution was then mixed with 19  $\mu$ L of 42mM Glycine and then vortexed at 25°C for 60 minutes in the dark. After centrifugation and washing with 1x PBS, GO-PEG-FITC was re-dispersed in 1 mL ddH<sub>2</sub>O. Cells were then incubated with GO-PEG-FITC (20  $\mu$ L) in 100  $\mu$ L of minimum essential medium for 6 hours. The medium was then removed, and the cells were washed with 1 mL of Hank's balanced salt solution and then fixed with fresh ethanol for 5 minutes at room temperature. The cells were washed three times with Hank's balanced salt solution and analyzed by a laser confocal microscope (Olympus FV10i).

## NPC Cell Culture

The NPC cell line TW01 was kindly provided by Dr. Lin CT (Department of Pathology and Graduate Institute of Pathology, College of Medicine, National Taiwan University, Taiwan). The cell line was derived from primary nasopharyngeal tumors of Chinese patients with de novo NPC.<sup>27,28</sup> The use of the NPC cell line was approved by the institutional review board of the Taipei Veterans General Hospital. The NPC cell line was maintained in DMEM with 10% FBS at 37°C under 5% CO<sub>2</sub>.

## In vitro Cytotoxicity Assay

Cell viability of the exposed cells was determined using the Cell Counting Kit-8 (Sigma-Aldrich, St. Louis, USA), according to the manufacturer's instructions. After seeding cells at a concentration of 2000 cells/well in 100  $\mu$ L

culture medium in a 96-well microplate for 24 hours, cells were washed with PBS twice and exposed with GO, GO-PEG, erlotinib, and GO-PEG-erlotinib for various concentrations in a humidified atmosphere (37°C and 5% CO<sub>2</sub>) for 2~3 days. Then, the cells were incubated with 10  $\mu$ L CCK-8 cell proliferation reagent for 2 hours. Optical density was measured using a microplate reader (Spectral Max250) at 450 nm.

## Wound Healing Assay

Cells were plated in 6-well plates. When the cells grew into full confluency, a wound was created on the monolayer cells by scraping a gap using a micropipette tip after cells had been treated with control and GO-PEG-erlotinib for 20 hours. The speed of wound closure was compared between GO-PEG-erlotinib treated groups and the control group. Photographs were taken under 100 $\times$  magnifications using phase contrast microscopy immediately after wound incision and at 20 hours later.

## Cell Invasion Assay

A Transwell cell culture chamber (Millipore, Bedford, MA, USA) with a 6.5-mm-diameter polycarbonate filter (8  $\mu$ m pore size) was coated with Matrigel, dried, and reconstituted at 37°C with culture medium. Culture medium containing 10% FBS was placed in the lower chamber (24-well plates). Then, the cells at  $1 \times 10^5$  cells per chamber were added to the upper chamber in serum-free DMEM. After 48 hours of incubation with control, GO-PEG, erlotinib or GO-PEG-erlotinib at 37°C, the suspended media in the lower chamber were removed. The cells that had invaded the lower side of the filter were fixed in methanol and stained with DAPI. The number of cells that passed through the pores into the lower chamber was counted under a fluorescent microscope (five fields per chamber).

## RNA-Seq Analysis

Total RNA from NPC cell lines treated with or without GO-PEG-erlotinib (2.15  $\mu$ g/mL) for 72 hours was extracted with RNeasy Mini Kit (Qiagen, Germany) according to the manufacturer's protocol. RNA was subjected to RNA-Seq analysis on BGISEQ-500 system by Tri-I Biotech, Inc. Briefly, the RNA was sheared and reverse transcribed using random primers to obtain cDNA used for library construction. We performed sequencing on prepared library<sup>29</sup> and filtered all the generated raw sequencing reads to get clean reads stored as

FASTQ format.<sup>30</sup> We used Bowtie2 and HISAT to map clean reads to reference genes and genome, respectively.<sup>31,32</sup> Gene expression level (FPKM) was quantified by RSEM.<sup>33</sup> We used the DEseq2 method to screen out differentially expressed genes between two groups with fold change  $\geq 2$  and adjusted P value  $\leq 0.05$ .<sup>34</sup> Gene ontology (GO) and pathway annotation and enrichment analyses were based on the GO Database (<http://www.geneontology.org/>) and KEGG pathway database (<http://www.genome.jp/kegg/>), respectively. We then used the Ingenuity Pathway Analysis (IPA) to assign biological functions to genes and network analysis using the Ingenuity Pathways Knowledge Base (Ingenuity Systems, Inc., Redwood City, CA, USA).

## Statistical Analysis

All experiments were carried out in triplicate, and at least three independent experiments were performed. The results are presented as the means  $\pm$  SDs. Statistical comparisons of multigroup data were analyzed by ANOVA, followed by Scheffé's post-test using SPSS 12.0 software (SPSS Inc. Chicago, IL). A value of  $p < 0.05$  indicated statistical significance.

## Results

We prepared GO and GO-PEG from the raw materials of graphite platelet followed the modified Hummers' method. We characterized the GO and GO-PEG using several tools, including the TEM, FTIR, DLS, and Raman spectroscopy. The TEM images showed the irregular morphology of GO and GO-PEG (Figure 1A) in the solution. Compared to GO-PEG, GO forms small clusters more readily in the solution. From the TEM images, GO-PEG showed better dispersibility in water. Moreover, no contaminating particles were found on the surface of both GO and GO-PEG, which revealed great purity of these two materials in the solution (data not shown). We further used the DSL to measure the size of GO and GO-PEG, which were 88 nm and 96 nm in average, respectively (Figure 1B). DLS is a technique in physics that can be used to determine the size-distribution profile of small particles in suspension or polymers in solution. The polydispersity index (PDI) is used to describe the degree of "non-uniformity" of a distribution. PDI between 0 and 0.35 means narrow size-distribution of particles. The PDI of GO and GO-PEG were 0.357 and 0.354, respectively. ZP (zeta potential) measurements represent the surface charge of the materials. The ZP of GO and GO-PEG were  $-42.1$  and  $-31.1$ ,

respectively (Figure 1B). The FTIR was used to obtain an infrared spectrum of absorption or emission of the GO and functionalized GO materials, which revealed that PEG was successfully conjugated on GO (Figure 1D). Raman spectroscopy was performed using a Micro-Raman Spectrometer (PTT-EL) equipped with a 532nm laser. Raman spectroscopy can provide substantial information about nanostructure defect type, domain size, impurity element, etc. A G-band at around  $1575\text{cm}^{-1}$  in the Raman spectra represents the  $\text{sp}^2$ -hybridized carbon structure of GO, while a D-band at around  $1355\text{cm}^{-1}$  appears when the carbon structure exhibits small defects or edges. The intensity ratio (intensity of the D-band/intensity of the G-band, ID/IG) represents the structural integrity of GO. GO and GO-PEG had similar ID/IG values, indicating that PEGylation did not destroy the aromatic structures of GO (Figure 1C and E). Absorbance of GO, GO-PEG, erlotinib, and GO-PEG-erlotinib analyzed by UV-Vis spectrophotometer is shown in Figure 1F.

We then conducted the drug loading and release studies, which are essential for evaluating a drug delivery system. The drug loading efficiency (LE) and encapsulation efficiency (EE) of erlotinib-loaded GO-PEG were about 80%, and 38%, respectively (Figure 2A). On average,  $46.5 \pm 9.58$   $\mu\text{g}$  erlotinib was loaded on  $141.39 \pm 9.45$   $\mu\text{g}$  GO-PEG when 200  $\mu\text{g}$  erlotinib was mixed with 200  $\mu\text{g}$  GO-PEG. In regard to drug release testing, the release rate of GO-PEG-erlotinib at pH 5 at 5 hours was 93.01%; at 24 hours was 95.88%; and at 72 hours was 98.99%. The release rate of GO-PEG-erlotinib at pH 7 at 5 hours was 63.38%; at 24 hours was 68.33%; and at 72 hours was 76.74% (Figure 2A). In order to duplicate the physiological temperature, a temperature of  $37^\circ\text{C}$  was selected for the drug release response. A pH of 7.4 corresponds to the physiological pH of normal cells, while a pH of 5.5 corresponds to acidic cancer environments, and also within endosomes after internalization. Figure 2B shows that the cumulative release profile of erlotinib from the GO-PEG is pH-dependent, in which erlotinib release is enhanced at pH 5.5.

To determine intracellular uptake of GO-PEG, NPC TW01 cells were cultured and incubated with FITC-labeled GO-PEG suspension for 6 hours. The identification of GO-PEG was made possible by the green fluorescence signals from FITC-labeled GO-PEG (Figure 3). The green fluorescence of FITC-labeled GO-PEG mostly appears in the cytoplasm of NPC TW01 cells. It is supposed that GO-PEG accumulating in the cytoplasm is via endocytosis.

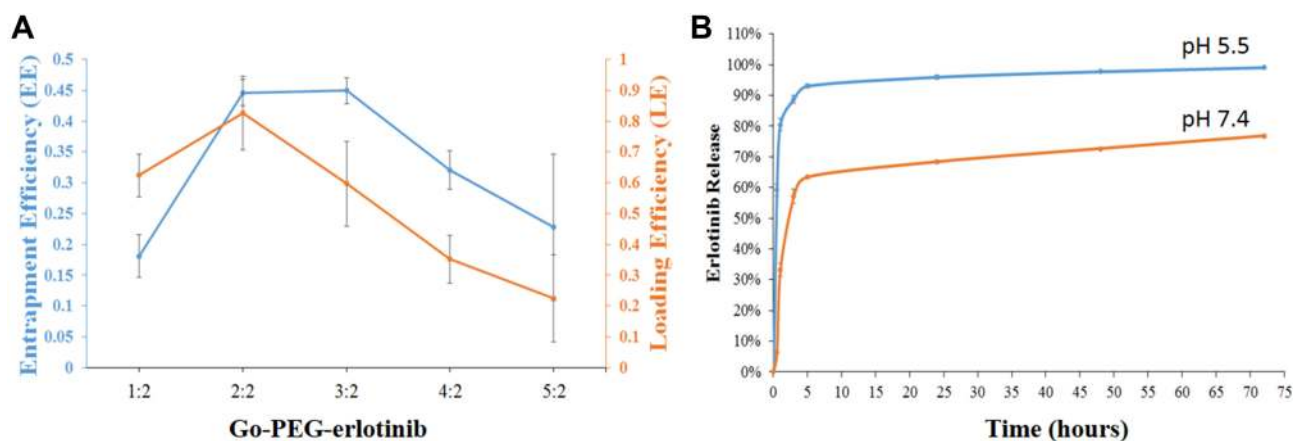


**Figure 2 (A)** The drug loading efficiency (LE) and encapsulation efficiency (EE) of erlotinib-loaded GO-PEG. **(B)** The drug release test of GO-PEG-erlotinib at pH 7.4 and 5.5.

We then tested the GO and GO-PEG on NPC cells. Both GO and GO-PEG showed mild cytotoxicity on NPC cells at a concentration below 10  $\mu\text{g}/\text{mL}$ . The erlotinib was further tested for cytotoxicity. Erlotinib seems to have little cytotoxicity effect on NPC cells; the  $\text{IC}_{50}$  at 72 hours is around 100  $\mu\text{g}/\text{mL}$  (data not shown). However, GO-PEG-erlotinib has great cytotoxicity with the  $\text{IC}_{50}$  at 72 hours being 2.12  $\mu\text{g}/\text{mL}$  (Figure 4). This indicates that GO-PEG might be a promising drug delivery vehicle for erlotinib in NPC treatment.

The migration of NPC TW01 cells with or without GO-PEG-erlotinib was assessed by a wound healing assay. More cells migrated to the denuded area of the wound in the control group than to the cells treated with 0.7 and 2.15  $\mu\text{g}/\text{mL}$  GO-PEG-erlotinib at 20 hours after the creation of the wound (Figure 5). The results indicated that GO-PEG-erlotinib inhibited the migration of NPC cells. To investigate whether GO-PEG-erlotinib could inhibit cell invasion, cell invasion assays were conducted. The number of migrating cells was significantly reduced after treatment with 2.15  $\mu\text{g}/\text{mL}$  GO-PEG-erlotinib (Figure 6).

To identify differentially expressed genes, the RNA-Seq of the NPC cell lines treated with and without 2.15  $\mu\text{g}/\text{mL}$  GO-PEG-erlotinib for 72 hours were compared. A p-value  $<0.05$  was considered statistically significant. In regard to GO-PEG-erlotinib, a total of 1455 genes were differentially expressed by at least two-fold, with 623 upregulated and

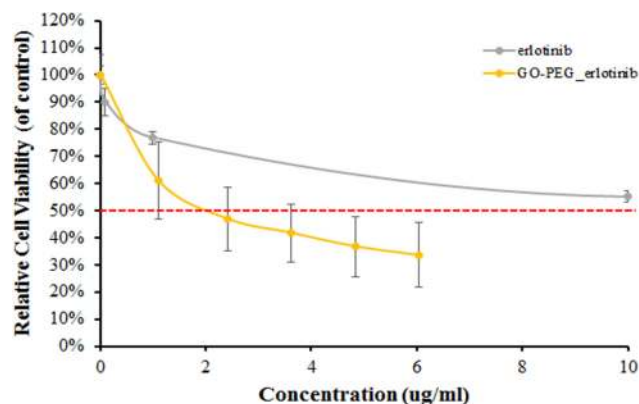


**Figure 4** Cell viability of NPC TW01 after treatment with erlotinib and GO-PEG-erlotinib at various concentrations. Cell viability was determined after incubating with erlotinib or GO-PEG-erlotinib for 72 hours.

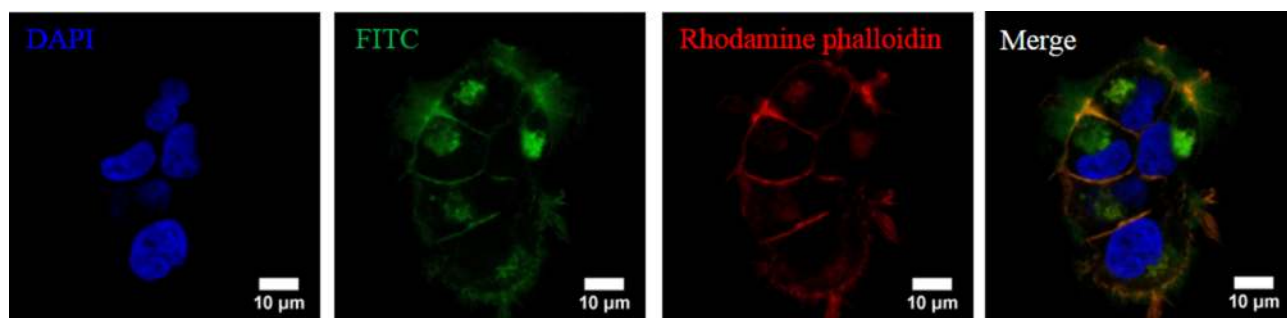


**Figure 3** Confocal microscopy images of NPC TW01 cells after treatment with FITC-labeled GO-PEG for 6 hours.

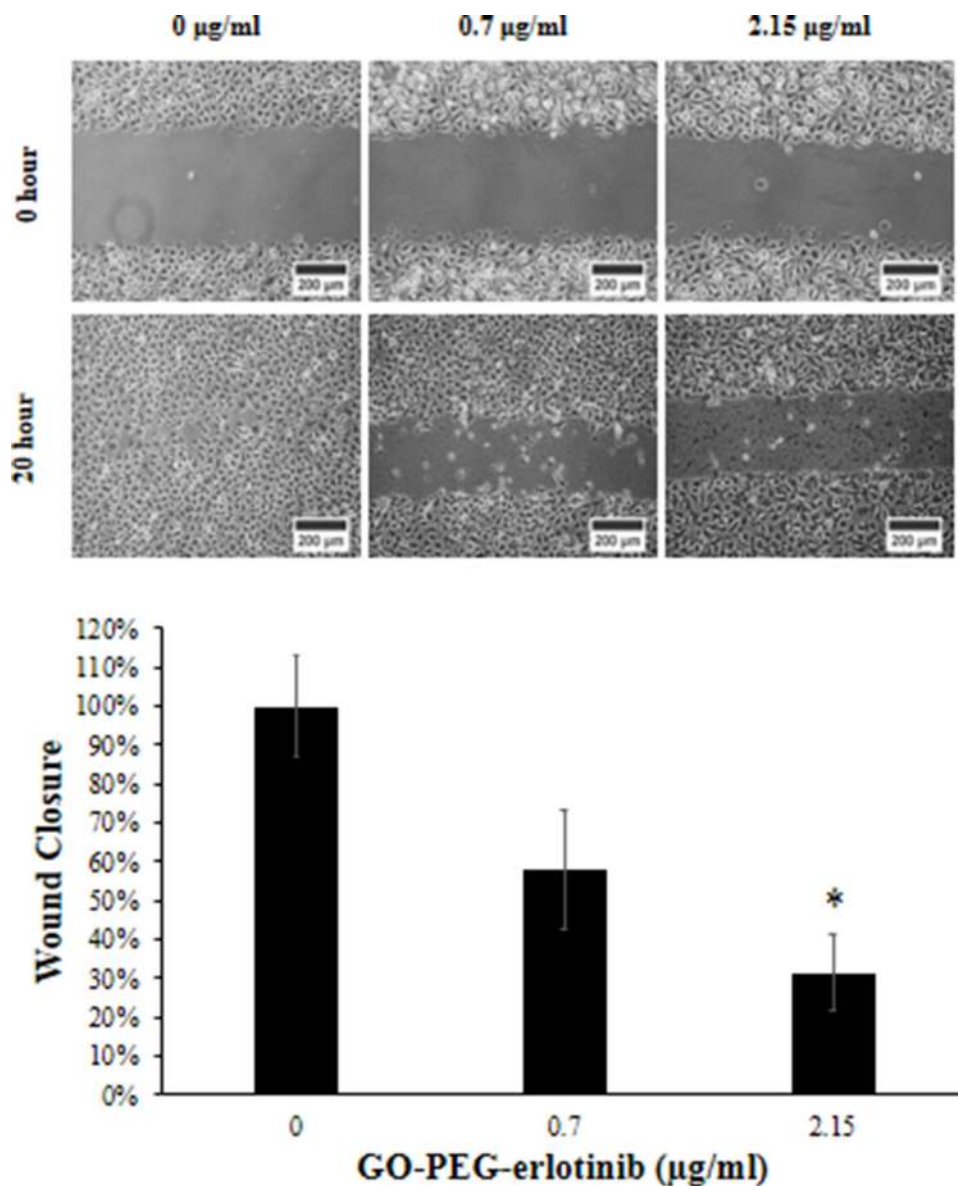


**Figure 5** GO-PEG-erlotinib reduces cell migration in NPC TW01 cells. More cells migrated to the denuded area of the wound in the control group (left) compared to the cells treated with 0.7 µg/mL GO-PEG-erlotinib (middle) and 2.15 µg/mL GO-PEG-erlotinib (right) at 20 hours after the creation of the wound. \* $p < 0.05$  compared with the control group by ANOVA.

832 downregulated genes. The data were then analyzed using the IPA functional analysis tool. Several networks and interactomes were created according to the biological functions of the genes and were ranked by the number of significantly expressed genes they contained. The top 10 upregulated and downregulated molecules and the top 10 upstream regulators in RNA-Seq analysis of NPC cells treated with GO-PEG-erlotinib are listed in Table 1. Further study of these top molecules will be conducted in the future to elucidate their roles in the mechanism of GO-PEG-erlotinib on NPC cells. Table 2 lists the top 5 associated networks of genes involved in the effect of GO-PEG-

erlotinib on NPC cells. Figure 7 shows the top-ranked network identified by IPA analysis in GO-PEG-erlotinib.

The KEGG pathway analysis of GO-PEG-Erlotinib on NPC cells is shown in Figure 8. There are seven branches for KEGG pathways: cellular processes, environmental information processing, genetic information processing, human disease (for animals only), metabolism, and organismal systems.

## Discussion

EGFR has been found to be overexpressed in 73% to 89% of NPC patients, which causes decreased overall

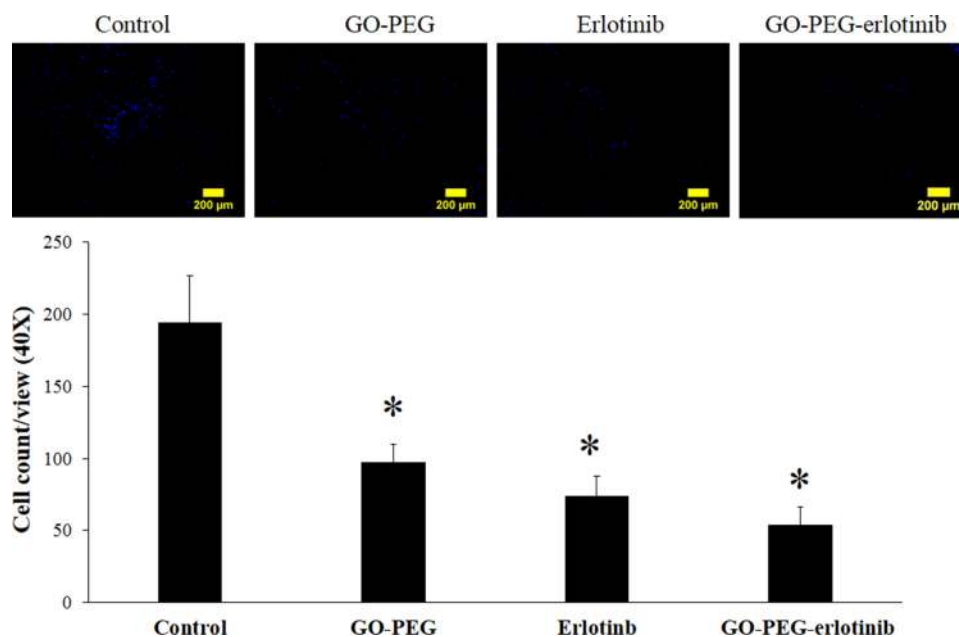


**Figure 6** GO-PEG-erlotinib inhibits cell invasion in NPC TW01 cells. Matrigel invasion assays of NPC TW01 cells showed that the invasion ability of NPC cells was reduced after treatment with 2.15 µg/mL GO-PEG-erlotinib, 2.15 µg/mL erlotinib, and 6.45 µg/mL GO-PEG for 48 hours. \* $p < 0.05$  compared with the control group by ANOVA.

survival and an increased risk of metastasis.<sup>35–37</sup> Several studies have shown that high EGFR expression is correlated with poor locoregional control and overall survival, but not distant metastasis-free survival (DMFS).<sup>38,39</sup> Erlotinib, an EGFR inhibitor, has been shown to be effective for NSCLC and pancreatic cancer, but without much study regarding its effect in head and neck cancer patients or in NPC patients.<sup>21</sup> A randomized phase II trial showed that the addition of erlotinib to cisplatin and radiotherapy did not confer additional tumor response or patient survival of 204 late-stage HNSCC patients.<sup>40</sup> Previously, a phase II trial conducted on patients with recurrent and/or metastatic NPC revealed

no efficacy of erlotinib as maintenance therapy after gemcitabine-platinum chemotherapy.<sup>23</sup>

Zheng et al recently identified serine protease inhibitor Kazal-type 6 (SPINK6) as a functional regulator of NPC metastasis via EGFR signaling, and erlotinib was revealed to reverse SPINK6-induced NPC cell migration and invasion in vitro, as well as inhibiting SPINK6-induced metastasis in vivo.<sup>41</sup> In our study, we found erlotinib has little cytotoxicity effect on NPC cells with the IC<sub>50</sub> at 72 hours being around 100 µg/mL, which may explain the relative unresponsiveness of erlotinib in clinical NPC patients. However, GO-PEG-erlotinib indeed showed good cytotoxicity on NPC cells with the IC<sub>50</sub> at 72 hours being

**Table 1** The Top 10 Upregulated and Downregulated Genes and Their Corresponding Upstream Regulators in RNA-Seq Analysis of NPC Cells Treated with GO-PEG-Erlotinib

Rank	Upregulated Gene	Expression Value	Downregulated Gene	Expression Value
1	<i>CHAC1</i>	4.279	<i>SNAIL</i>	-4.054
2	<i>RGPD4</i>	3.225	<i>ART5</i>	-3.982
3	<i>KRCC1</i>	3.046	<i>NPTX1</i>	-3.880
4	<i>ELAC1</i>	2.941	<i>HIST1H2BJ</i>	-3.774
5	<i>BORCS8-MEF2B</i>	2.755	<i>ART1</i>	-3.474
6	<i>CYP1A1</i>	2.755	<i>SLC6A12</i>	-3.434
7	<i>FGFBP3</i>	2.592	<i>SLC17A7</i>	-3.313
8	<i>C7orf25</i>	2.576	<i>KCNE1B</i>	-3.311
9	<i>SPRN</i>	2.483	<i>KLHL41</i>	-3.261
10	<i>MAGI2</i>	2.478	<i>SUCNR1</i>	-3.232



**Table 2** The Top 5 Associated Networks Involved in the Effect of GO-PEG-Erlotinib on NPC Cells Identified by IPA

Rank	Molecules	Associated Network Functions
1	34	Cardiovascular Disease, Hematological Disease, Hereditary Disorder
2	34	Cellular Development, Embryonic Development, Hair and Skin Development and Function
3	32	Cell Death and Survival, Cell-mediated Immune Response, Cellular Function and Maintenance
4	31	Reproductive System Development and Function, Cancer, Organismal Injury and Abnormalities
5	31	Endocrine System Development and Function, Molecular Transport, Small Molecule Biochemistry

2.12 ug/mL. We calculated the drug LE and EE of erlotinib-loaded GO-PEG was about 80%, and 38%, respectively, and the release rate of GO-PEG-erlotinib was enhanced at pH 5.5, corresponding to the acidic cancer environments in endosomes after internalization. Most tumor cells have high metabolic activity, which contributes to their more acidic intracellular pH.<sup>42</sup> Thus, an internalized graphene-based drug with pH-responsive characteristics, like GO-PEG-erlotinib in our study, can specifically release the drug at tumor sites.<sup>11</sup> Moreover, our results

show that GO-PEG-erlotinib not only reduced NPC cell viability in a dose-dependent manner but also inhibited the migration and invasion of NPC cells. The relatively moderate drug loading and the pH-sensitive release of erlotinib suggest that GO-PEG is a potential drug delivery vehicle for cancer therapy,<sup>43,44</sup> and that GO-PEG is a promising drug delivery vehicle for erlotinib in NPC treatment.

Graphene-based materials immobilize various biomolecules through either noncovalent adsorption, such as  $\pi$ - $\pi$  stacking, hydrogen bonds, and electrostatic interaction; or

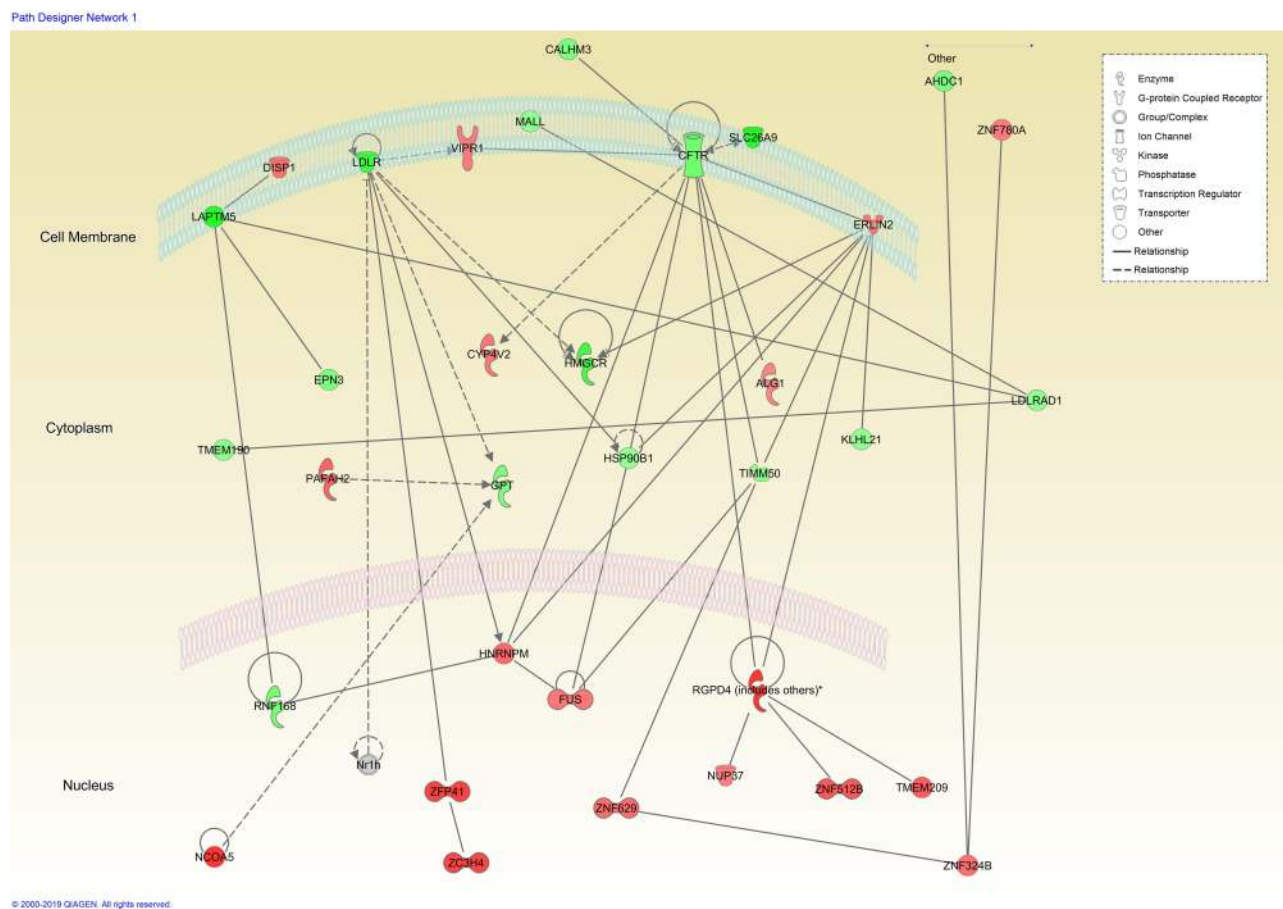


**Figure 7** The top-ranked network identified by IPA analysis in GO-PEG-erlotinib study. The top-ranked network, which includes 34 genes, is related to cardiovascular disease, hematological disease, and hereditary disorder. The genes shaded in red are upregulated, and genes shaded in green are downregulated. All shaded genes are statistically significant, as indicated by the statistical analysis. A dotted line indicates an indirect interaction between the two gene products, and a solid line represents a direct interaction.

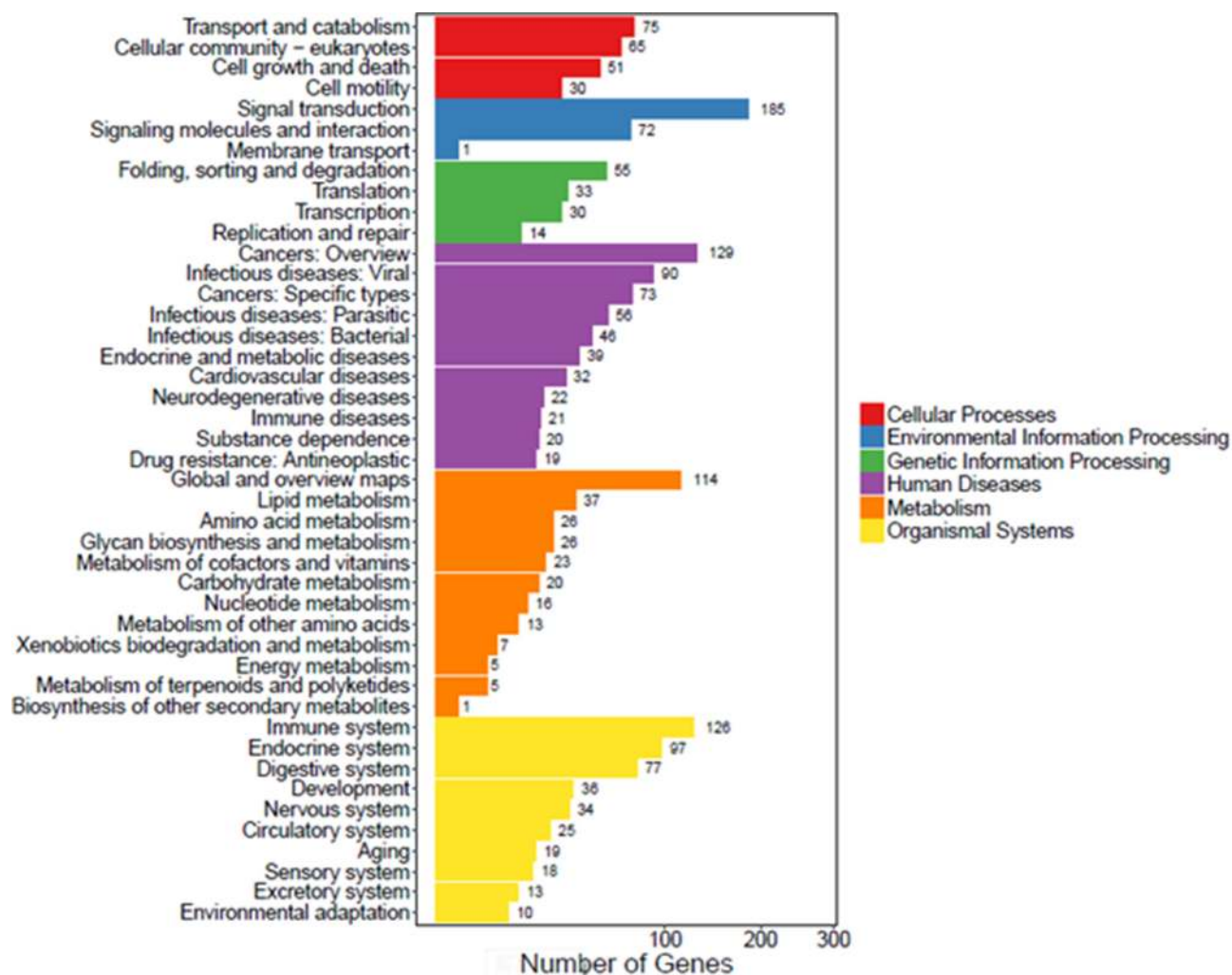


**Figure 8** KEGG pathway analysis of GO-PEG-erlotinib on NPC cells. There are seven branches for KEGG pathways: cellular processes, environmental information processing, genetic information processing, human disease, metabolism, and organismal systems.

covalent binding by their enriched oxygen functional groups.<sup>15</sup> They offer a high surface to weight ratio, a high possibility for surface modification, high drug-loading efficiency, a pH-responsive drug-delivery mechanism, and photothermal effects compared to other drug delivery systems.<sup>18,45,46</sup> Graphene is characterized by a pure carbon, an aromatic network providing an open surface for noncovalent interaction with biomolecules, while GO has many epoxides, carboxyl, and hydroxyl groups on its basal plane and edges which can bind with biomolecules via covalent, electrostatic, and hydrogen bond interactions.<sup>43,44</sup>

Most drugs binding on GO are based on noncovalent interactions. For example, chemotherapeutic drugs possessing aromatic ring structures, such as doxorubicin, camptothecin, and SN-38, bind on GO through  $\pi$ - $\pi$  stacking.<sup>47</sup> Various methods have been developed to

functionalize GO for improving its drug carrier function. Lui et al found that GO functionalized with polyethylene glycol (PEG) can carry water-insoluble cancer drugs such as camptothecin and SN38 and showed pH-dependent drug release behavior.<sup>48</sup> Besides, functionalized GO can enter mammalian cells, and thus it is a reasonable drug carrier. Moreover, the hydrophilic groups on both sides of GO make it stable in physiologic solutions while carrying drugs. In our study, intracellular uptake of FITC-labeled GO-PEG in NPC cells was clearly observed under confocal microscopy, which suggested that GO-PEG accumulating in the cytoplasm is via endocytosis. Finally, GO-PEG-erlotinib showed much better cytotoxicity on NPC cells than erlotinib alone, demonstrating that GO-PEG is a promising drug carrier for possible usage in NPC treatment in the future.

In recent years, several studies have focused on graphene and its derivatives as potential drug carriers for cancer therapy. Yang et al used a chemical coprecipitation method, not only adding Fe<sub>3</sub>O<sub>4</sub> magnetic nanoparticles onto graphene but also decorating it with folic acid as a targeting ligand. The drug-loaded graphene selectively killed breast cancer cells with released doxorubicin.<sup>45</sup> Zhang et al designed the drug carrier with low drug resistance rate but high cytotoxic efficacy by adding positive-charged polyethylenimine (PEI) onto the doxorubicin-loaded graphene which can adsorb negative-charged Bcl-2 siRNA.<sup>49</sup> Lu et al modified the GO surface with abundant polyacrylic acid (PAA) chains, which can react with BCNU through carbodiimide-mediated amide bond formation to increase drug loading. The PAA-GO-BCNU showed promising anticancer efficacy in *in vitro* study.<sup>47</sup> Yin et al functionalized GO with PEI and (PEG) as a plasmid-based Stat3 siRNA carrier, which showed a significant regression in tumor growth and tumor weight of mouse malignant melanoma growth *in vivo*.<sup>50</sup> Yang et al developed epidermal growth factor receptor (EGFR) antibody-conjugated PEGylated nanographene oxide (PEG-NGO) carrying epirubicin (EPI) that was able to target the tumor and kill the cancer cells by its triple-therapeutics (growth signal blocking, chemotherapy, photothermal therapy). The synergistic-targeted treatment simultaneously enhances the local drug concentration and performs ultra-efficient tumor suppression to significantly prolong survival in mice. This novel drug delivery platform overcomes the problems of low accumulation of most chemotherapeutic agents in tumor tissue and multidrug resistance (MDR) in current cancer treatment.<sup>51</sup> Recently, Pei et al developed cisplatin and doxorubicin dual-drug-loaded PEGylated nano-graphene oxide which exhibited significantly increased anticancer effect than the single drug delivery system.<sup>52</sup> Wang et al synthesized folate-modified GO/PEI siRNA nanocomplexes which successfully targeted ovarian cancer cells *in vitro*.<sup>53</sup> Shirvalilou et al developed magnetic NGO as a drug carrier for improving glioma-targeted iodo-2-deoxyuridine (IUdR) delivery and imaging.<sup>54</sup>

By conducting RNA-Seq analysis and following IPA analysis, the top 10 upregulated and top 10 downregulated molecules after GO-PEG-erlotinib treatment on NPC cells were identified (Table 1). Some of these molecules have been reported to be associated with carcinogenesis and prognosis in other types of cancers. CHAC1 (ChaC glutathione-specific gamma-glutamylcyclotransferase 1) plays a role in the regulation of glutathione levels and oxidative

balance in cells and is also a proapoptotic component of the unfolded protein response (UPR).<sup>55,56</sup> Activation of CHAC1 has been reported to induce cell apoptosis and decrease cell proliferation in human head and neck squamous cell cancer cell lines.<sup>57</sup> CYP1A1 (cytochrome P450 family 1 subfamily A member 1) is located at the endoplasmic reticulum. It can metabolize some polycyclic aromatic hydrocarbons to carcinogenic intermediates. This gene has been found to be associated with lung, prostate, and cervical cancer risks.<sup>58–60</sup> SNAI1 (snail family transcriptional repressor 1) proteins primarily act as transcriptional repressors.<sup>61</sup> It can induce epithelial-to-mesenchymal transition (EMT) in colorectal and lung cancer cells.<sup>62,63</sup> NPTX1 (neuronal pentraxin 1) belongs to the long pentraxin family of protein and is highly expressed in the central nervous system.<sup>64</sup> It is also involved in the regulation of apoptosis in some types of cells.<sup>65,66</sup> Recently, some studies found that NPTX1 may be involved in the progression of lung, pancreatic, and colon cancers.<sup>67–69</sup>

Recently, several ligands have been used in cancer targeted therapies, such as biotin, transferrin, and folate.<sup>70,71</sup> Montazerabadi et al functionalized curcumin-loaded dendritic magnetite nanocarriers with folate, which generated a thermo-chemotherapeutic effect on folate receptor-expressed cancer cells.<sup>72</sup> Zeiniazade et al used folate-conjugated gold nanoparticles for targeted nano-photo-thermal therapy.<sup>73</sup> Because of the high surface-area-to-volume ratio of nanocarriers, designing novel drug carriers with multiple targeting ligands are feasible ways to increase their antitumor effect.<sup>71</sup> In the future, we will further modify GO-PEG-erlotinib with specific ligands to induce selective cancer cell death.

Our study revealed that GO-PEG is a promising drug carrier for erlotinib with the advantages of high drug loading and pH-dependent controlled release. GO-PEG-erlotinib reduced NPC cell viability in a dose-dependent manner, and also inhibited the migration and invasion of NPC cells. The RNA sequencing revealed important molecules and several related molecular mechanisms. Further studies will be needed in the future.

## Conclusion

GO-PEG-erlotinib effectively suppressed NPC cell proliferation, migration, and invasion, and presented a better anticancer effect than free drugs. Several molecules and mechanisms were involved. GO-PEG-erlotinib may be a potential therapeutic agent for treating NPC in the future.

## Acknowledgments

This research was supported by grants from the Ministry of Science and Technology (MOST106-2314-B-075-035-MY3-2) to MYL and (MOST107-2314-B-182-020) to YJL. The authors thank the Clinical Research Core Laboratory at Taipei Veterans General Hospital for facility support.

## Disclosure

The authors report no conflicts of interest for this work.

## References

1. Cho WC. Nasopharyngeal carcinoma: molecular biomarker discovery and progress. *Mol Cancer*. 2007;6:1.
2. Lu JJ, Cooper JS, Lee AW. *Nasopharyngeal Cancer: Multidisciplinary Management*. Springer Science & Business Media; 2010.
3. Tao Q, Chan AT. Nasopharyngeal carcinoma: molecular pathogenesis and therapeutic developments. *Expert Rev Mol Med*. 2007;9(12):1–24.
4. Chou J, Lin YC, Kim J, et al. Nasopharyngeal carcinoma—review of the molecular mechanisms of tumorigenesis. *Head Neck*. 2008;30(7):946–963. doi:10.1002/hed.20833
5. Lee YC, Hwang YC, Chen KC, et al. Effect of Epstein-Barr virus infection on global gene expression in nasopharyngeal carcinoma. *Funct Integr Genomics*. 2007;7(1):79–93. doi:10.1007/s10142-006-0035-2
6. Chen X, Liang S, Zheng W, Liao Z, Shang T, Ma W. Meta-analysis of nasopharyngeal carcinoma microarray data explores mechanism of EBV-regulated neoplastic transformation. *BMC Genomics*. 2008;9:322. doi:10.1186/1471-2164-9-322
7. Bruce JP, Yip K, Bratman SV, Ito E, Liu FF. Nasopharyngeal cancer: molecular landscape. *J Clin Oncol*. 2015;33(29):3346–3355. doi:10.1200/JCO.2015.60.7846
8. Dai W, Zheng H, Cheung AK, Lung ML. Genetic and epigenetic landscape of nasopharyngeal carcinoma. *China Clin Oncol*. 2016;5(2):16. doi:10.21037/cco.2016.03.06
9. Gooi Z, Richmon J, Agrawal N, et al. AHNS series - Do you know your guidelines? Principles of treatment for nasopharyngeal cancer: a review of the national comprehensive cancer network guidelines. *Head Neck*. 2017;39(2):201–205. doi:10.1002/hed.24635
10. Ghanbarzadeh S, Hamishehkar H. Application of graphene and its derivatives in cancer diagnosis and treatment. *Drug Res (Stuttg)*. 2017;67(12):681–687. doi:10.1055/s-0042-115638
11. Gu Z, Zhu S, Yan L, Zhao F, Zhao Y. Graphene-based smart platforms for combined cancer therapy. *Adv Mater*. 2019;31(9):e1800662. doi:10.1002/adma.201800662
12. Liu J, Dong J, Zhang T, Peng Q. Graphene-based nanomaterials and their potentials in advanced drug delivery and cancer therapy. *J Control Release*. 2018;286:64–73. doi:10.1016/j.jconrel.2018.07.034
13. de Melo-diogo D, Lima-Sousa R, Alves CG, Costa EC, Louro RO, Correia IJ. Functionalization of graphene family nanomaterials for application in cancer therapy. *Colloids Surf B Biointerfaces*. 2018;171:260–275. doi:10.1016/j.colsurfb.2018.07.030
14. Novoselov KS, Geim AK, Morozov SV, et al. Electric field effect in atomically thin carbon films. *Science*. 2004;306(5696):666–669. doi:10.1126/science.1102896
15. Li D, Zhang W, Yu X, Wang Z, Su Z, Wei G. When biomolecules meet graphene: from molecular level interactions to material design and applications. *Nanoscale*. 2016;8(47):19491–19509. doi:10.1039/C6NR07249F
16. Gurunathan S, Kim JH. Synthesis, toxicity, biocompatibility, and biomedical applications of graphene and graphene-related materials. *Int J Nanomedicine*. 2016;11:1927–1945.
17. Rahmanian N, Eskandani M, Barar J, Omid Y. Recent trends in targeted therapy of cancer using graphene oxide-modified multifunctional nanomedicines. *J Drug Target*. 2017;25(3):202–215.
18. Yang K, Feng L, Liu Z. Stimuli responsive drug delivery systems based on nano-graphene for cancer therapy. *Adv Drug Deliv Rev*. 2016;105(Pt B):228–241. doi:10.1016/j.addr.2016.05.015
19. Zhang B, Wang Y, Zhai G. Biomedical applications of the graphene-based materials. *Mater Sci Eng C Mater Biol Appl*. 2016;61:953–964. doi:10.1016/j.msec.2015.12.073
20. Gulzar A, Yang P, He F, et al. Bioapplications of graphene constructed functional nanomaterials. *Chem Biol Interact*. 2017;262:69–89. doi:10.1016/j.cbi.2016.11.019
21. Xu MJ, Johnson DE, Grandis JR. EGFR-targeted therapies in the post-genomic era. *Cancer Metastasis Rev*. 2017;36(3):463–473. doi:10.1007/s10555-017-9687-8
22. Zhang HH, Yuan TZ, Li J, et al. Erlotinib: an enhancer of radiation therapy in nasopharyngeal carcinoma. *Exp Ther Med*. 2013;6(4):1062–1066. doi:10.3892/etm.2013.1245
23. You B, Le Tourneau C, Chen EX, et al. A Phase II trial of erlotinib as maintenance treatment after gemcitabine plus platinum-based chemotherapy in patients with recurrent and/or metastatic nasopharyngeal carcinoma. *Am J Clin Oncol*. 2012;35(3):255–260. doi:10.1097/JCO.0b013e31820dbdce
24. Lan MY, Chen CL, Lin KT, et al. From NPC therapeutic target identification to potential treatment strategy. *Mol Cancer Ther*. 2010;9(9):2511–2523.
25. Lan MY, Yang WL, Lin KT, et al. Using computational strategies to predict potential drugs for nasopharyngeal carcinoma. *Head Neck*. 2014;36(10):1398–1407.
26. Hummers Jr WS, Offeman RE. Preparation of graphitic oxide. *J Am Chem Soc*. 1958;80(6):1339.
27. Lin CT, Wong CI, Chan WY, et al. Establishment and characterization of two nasopharyngeal carcinoma cell lines. *Lab Invest*. 1990;62(6):713–724.
28. Lin CT, Chan WY, Chen W, et al. Characterization of seven newly established nasopharyngeal carcinoma cell lines. *Lab Invest*. 1993;68(6):716–727.
29. Huang J, Liang X, Xuan Y, et al. A reference human genome dataset of the BGISEQ-500 sequencer. *Gigascience*. 2017;6(5):1–9.
30. Cock PJ, Fields CJ, Goto N, Heuer ML, Rice PM. The Sanger FASTQ file format for sequences with quality scores, and the Solexa/Illumina FASTQ variants. *Nucleic Acids Res*. 2010;38(6):1767–1771.
31. Kim D, Langmead B, Salzberg SL. HISAT: a fast spliced aligner with low memory requirements. *Nat Methods*. 2015;12(4):357–360. doi:10.1038/nmeth.3317
32. Langmead B, Salzberg SL. Fast gapped-read alignment with Bowtie 2. *Nat Methods*. 2012;9(4):357–359. doi:10.1038/nmeth.1923
33. Su CY, Fu D, Lu AY, et al. Transfer printing of graphene strip from the graphene grown on copper wires. *Nanotechnology*. 2011;22(18):185309. doi:10.1088/0957-4484/22/18/185309
34. Love MI, Huber W, Anders S. Moderated estimation of fold change and dispersion for RNA-seq data with DESeq2. *Genome Biol*. 2014;15(12):550.
35. Chua DT, Nicholls JM, Sham JS, Au GK. Prognostic value of epidermal growth factor receptor expression in patients with advanced stage nasopharyngeal carcinoma treated with induction chemotherapy and radiotherapy. *Int J Radiat Oncol Biol Phys*. 2004;59(1):11–20. doi:10.1016/j.ijrobp.2003.10.038
36. Sheen TS, Huang YT, Chang YL, et al. Epstein-Barr virus-encoded latent membrane protein 1 co-expresses with epidermal growth factor receptor in nasopharyngeal carcinoma. *Jpn J Cancer Res*. 1999;90(12):1285–1292. doi:10.1111/j.1349-7006.1999.tb00710.x

37. Ma BB, Poon TC, To KF, et al. Prognostic significance of tumor angiogenesis, Ki 67, p53 oncoprotein, epidermal growth factor receptor and HER2 receptor protein expression in undifferentiated nasopharyngeal carcinoma—a prospective study. *Head Neck*. 2003;25(10):864–872. doi:10.1002/hed.10307
38. Ooft ML, Braunius WW, Heus P, et al. Prognostic significance of the EGFR pathway in nasopharyngeal carcinoma: a systematic review and meta-analysis. *Biomark Med*. 2015;9(10):997–1010. doi:10.2217/bmm.15.68
39. Sun W, Long G, Wang J, Mei Q, Liu D, Hu G. Prognostic role of epidermal growth factor receptor in nasopharyngeal carcinoma: a meta-analysis. *Head Neck*. 2014;36(10):1508–1516.
40. Martins RG, Parvathaneni U, Bauman JE, et al. Cisplatin and radiotherapy with or without erlotinib in locally advanced squamous cell carcinoma of the head and neck: a randomized phase II trial. *J Clin Oncol*. 2013;31(11):1415–1421. doi:10.1200/JCO.2012.46.3299
41. Zheng LS, Yang JP, Cao Y, et al. SPINK6 promotes metastasis of nasopharyngeal carcinoma via binding and activation of epithelial growth factor receptor. *Cancer Res*. 2017;77(2):579–589. doi:10.1158/0008-5472.CAN-16-1281
42. Kato Y, Ozawa S, Miyamoto C, et al. Acidic extracellular microenvironment and cancer. *Cancer Cell Int*. 2013;13(1):89. doi:10.1186/1475-2867-13-89
43. Zhu Y, Murali S, Cai W, et al. Graphene and graphene oxide: synthesis, properties, and applications. *Adv Mater*. 2010;22(35):3906–3924.
44. Wang Y, Li Z, Wang J, Li J, Lin Y. Graphene and graphene oxide: biofunctionalization and applications in biotechnology. *Trends Biotechnol*. 2011;29(5):205–212. doi:10.1016/j.tibtech.2011.01.008
45. Yang X, Wang Y, Huang X, et al. Multi-functionalized graphene oxide based anticancer drug-carrier with dual-targeting function and pH-sensitivity. *J Mater Chem*. 2011;21(10):3448–3454. doi:10.1039/C0JM02494E
46. Yang K, Zhang S, Zhang G, Sun X, Lee ST, Liu Z. Graphene in mice: ultrahigh in vivo tumor uptake and efficient photothermal therapy. *Nano Lett*. 2010;10(9):3318–3323. doi:10.1021/nl100996u
47. Lu YJ, Yang HW, Hung SC, et al. Improving thermal stability and efficacy of BCNU in treating glioma cells using PAA-functionalized graphene oxide. *Int J Nanomedicine*. 2012;7:1737–1747.
48. Liu Z, Robinson JT, Sun X, Dai H. PEGylated nanographene oxide for delivery of water-insoluble cancer drugs. *J Am Chem Soc*. 2008;130(33):10876–10877.
49. Zhang L, Lu Z, Zhao Q, Huang J, Shen H, Zhang Z. Enhanced chemotherapy efficacy by sequential delivery of siRNA and anticancer drugs using PEI-grafted graphene oxide. *Small*. 2011;7(4):460–464. doi:10.1002/sml.201001522
50. Yin D, Li Y, Lin H, et al. Functional graphene oxide as a plasmid-based Stat3 siRNA carrier inhibits mouse malignant melanoma growth in vivo. *Nanotechnology*. 2013;24(10):105102. doi:10.1088/0957-4484/24/10/105102
51. Yang HW, Lu YJ, Lin KJ, et al. EGRF conjugated PEGylated nanographene oxide for targeted chemotherapy and photothermal therapy. *Biomaterials*. 2013;34(29):7204–7214. doi:10.1016/j.biomaterials.2013.06.007
52. Pei X, Zhu Z, Gan Z, et al. PEGylated nano-graphene oxide as a nanocarrier for delivering mixed anticancer drugs to improve anticancer activity. *Sci Rep*. 2020;10(1):2717. doi:10.1038/s41598-020-59624-w
53. Wang Y, Sun G, Gong Y, Zhang Y, Liang X, Yang L. Functionalized folate-modified graphene oxide/PEI siRNA nanocomplexes for targeted ovarian cancer gene therapy. *Nanoscale Res Lett*. 2020;15(1):57. doi:10.1186/s11671-020-3281-7
54. Shirvalilou S, Khoei S, Khoee S, Raoufi NJ, Karimi MR, Shakeri-Zadeh A. Development of a magnetic nano-graphene oxide carrier for improved glioma-targeted drug delivery and imaging: in vitro and in vivo evaluations. *Chem Biol Interact*. 2018;295:97–108. doi:10.1016/j.cbi.2018.08.027
55. Mungrue IN, Pagnon J, Kohannim O, Gargalovic PS, Lusis AJ. CHAC1/MGC4504 is a novel proapoptotic component of the unfolded protein response, downstream of the ATF4-ATF3-CHOP cascade. *J Immunol*. 2009;182(1):466–476. doi:10.4049/jimmunol.182.1.466
56. Crawford RR, Prescott ET, Sylvester CF, et al. Human CHAC1 protein degrades glutathione, and mRNA induction is regulated by the transcription factors ATF4 and ATF3 and a Bipartite ATF/CRE regulatory element. *J Biol Chem*. 2015;290(25):15878–15891.
57. Joo NE, Ritchie K, Kamarajan P, Miao D, Kapila YL. Nisin, an apoptogenic bacteriocin and food preservative, attenuates HNSCC tumorigenesis via CHAC1. *Cancer Med*. 2012;1(3):295–305. doi:10.1002/cam4.35
58. Liu Y, Li X, Zhang B, et al. CYP1A1 methylation mediates the effect of smoking and occupational polycyclic aromatic hydrocarbons co-exposure on oxidative DNA damage among Chinese coke-oven workers. *Environ Health*. 2019;18(1):69. doi:10.1186/s12940-019-0508-0
59. Zhu W, Liu H, Wang X, et al. Associations of CYP1 polymorphisms with risk of prostate cancer: an updated meta-analysis. *Biosci Rep*. 2019;39(3). doi:10.1042/BSR20181876.
60. Sengupta D, Guha U, Mitra S, Ghosh S, Bhattacharjee S, Sengupta M. Meta-analysis of polymorphic variants conferring genetic risk to cervical cancer in Indian women supports CYP1A1 as an important associated locus. *Asian Pac J Cancer Prev*. 2018;19(8):2071–2081.
61. Jagle S, Busch H, Freihen V, et al. SNAIL1-mediated downregulation of FOXA proteins facilitates the inactivation of transcriptional enhancer elements at key epithelial genes in colorectal cancer cells. *PLoS Genet*. 2017;13(11):e1007109. doi:10.1371/journal.pgen.1007109
62. Ye X, Tam WL, Shibue T, et al. Distinct EMT programs control normal mammary stem cells and tumour-initiating cells. *Nature*. 2015;525(7568):256–260. doi:10.1038/nature14897
63. You J, Li M, Cao LM, et al. Snail1-dependent cancer-associated fibroblasts induce epithelial-mesenchymal transition in lung cancer cells via exosomes. *QJM*. 2019;112(8):581–590. doi:10.1093/qjmed/hcz093
64. Schlimgen AK, Helms JA, Vogel H, Perin MS. Neuronal pentraxin, a secreted protein with homology to acute phase proteins of the immune system. *Neuron*. 1995;14(3):519–526. doi:10.1016/0896-6273(95)90308-9
65. Schvartz D, Coute Y, Brunner Y, Wollheim CB, Sanchez JC. Modulation of neuronal pentraxin 1 expression in rat pancreatic beta-cells submitted to chronic glucotoxic stress. *Mol Cell Proteomics*. 2012;11(8):244–254. doi:10.1074/mcp.M112.018051
66. Guzeloglu-Kayisli O, Basar M, Shapiro JP, et al. Long-acting progestin-only contraceptives enhance human endometrial stromal cell expressed neuronal pentraxin-1 and reactive oxygen species to promote endothelial cell apoptosis. *J Clin Endocrinol Metab*. 2014;99(10):E1957–1966. doi:10.1210/jc.2014-1770
67. Zhou C, Qin Y, Xie Z, et al. NPTX1 is a novel epigenetic regulation gene and associated with prognosis in lung cancer. *Biochem Biophys Res Commun*. 2015;458(2):381–386. doi:10.1016/j.bbrc.2015.01.124
68. Yue W, Wang T, Zachariah E, et al. Transcriptomic analysis of pancreatic cancer cells in response to metformin and aspirin: an implication of synergy. *Sci Rep*. 2015;5:13390. doi:10.1038/srep13390
69. Mori Y, Oлару AV, Cheng Y, et al. Novel candidate colorectal cancer biomarkers identified by methylation microarray-based scanning. *Endocr Relat Cancer*. 2011;18(4):465–478. doi:10.1530/ERC-11-0083
70. Mehdizadeh A, Pandesh S, Shakeri-Zadeh A, et al. The effects of folate-conjugated gold nanorods in combination with plasmonic photothermal therapy on mouse epidermal carcinoma cells. *Lasers Med Sci*. 2014;29(3):939–948. doi:10.1007/s10103-013-1414-2

71. Pérez-Herrero E, Fernández-Medarde A. Advanced targeted therapies in cancer: drug nanocarriers, the future of chemotherapy. *Eur J Pharm Biopharm.* 2015;93:52–79. doi:10.1016/j.ejpb.2015.03.018
72. Montazerabadi A, Beik J, Irajirad R, et al. Folate-modified and curcumin-loaded dendritic magnetite nanocarriers for the targeted thermo-chemotherapy of cancer cells. *Artif Cells Nanomed Biotechnol.* 2019;47(1):330–340. doi:10.1080/21691401.2018.1557670
73. Zeinizade E, Tabei M, Shakeri-Zadeh A, et al. Selective apoptosis induction in cancer cells using folate-conjugated gold nanoparticles and controlling the laser irradiation conditions. *Artif Cells Nanomed Biotechnol.* 2018;46(sup1):1026–1038. doi:10.1080/21691401.2018.1443116

## International Journal of Nanomedicine

Dovepress

### Publish your work in this journal

The International Journal of Nanomedicine is an international, peer-reviewed journal focusing on the application of nanotechnology in diagnostics, therapeutics, and drug delivery systems throughout the biomedical field. This journal is indexed on PubMed Central, MedLine, CAS, SciSearch®, Current Contents®/Clinical Medicine,

Journal Citation Reports/Science Edition, EMBase, Scopus and the Elsevier Bibliographic databases. The manuscript management system is completely online and includes a very quick and fair peer-review system, which is all easy to use. Visit <http://www.dovepress.com/testimonials.php> to read real quotes from published authors.

Submit your manuscript here: <https://www.dovepress.com/international-journal-of-nanomedicine-journal>